J. Fluid Mech. (1992), *vol.* 242, *pp.* 31–50
Printed in Great Britain

The slow-drift motion of arrays of vertical cylinders

By O. J. EMMERHOFF AND P. D. SCLAVOUNOS
Department of Ocean Engineering, Massachusetts Institute of Technology, Cambridge, MA 02139, USA

(Received 4 November 1991 and in revised form 3 February 1992)

The large-amplitude rectilinear 'slow-drift' oscillation of a floating body constrained by a weak restoring force in random waves is considered. The free-surface flow is approximated by a perturbation series expansion for a small slow-drift velocity and wave steepness. A model slow-drift equation of motion is derived, the time-dependent slow-drift excitation force and wave damping coefficient are defined and the complete series of free-surface problems governing their magnitude are formulated. The free-surface problem governing the wave-drift damping coefficient in monochromatic waves is studied and an explicit solution is obtained for a vertical circular cylinder of infinite draught. This solution is extended for arrays of vertical circular cylinders by employing an exact interaction theory. The wave-drift damping coefficient is evaluated for configurations of interest in practice and an expression is derived for the steady drifting velocity of an unconstrained body in regular waves.

1. Introduction

Compliant offshore structures floating in ambient waves may undergo large-amplitude 'slow-drift' oscillations about their mean position when constrained by weak restoring forces. The modelling and prediction of such excursions is of evident importance for the design of the structure subsystems (i.e. mooring lines, risers, tethers) and have been the subject of a number of theoretical studies.

The characteristic period of 'slow' horizontal oscillations of offshore structures constrained by mooring or tether systems is typically large relative to the period of the 'fast' oscillatory responses induced by linear wave effects and restored by hydrostatic forces. This disparity of periods suggests the study of the slow-drift oscillation problem under the assumption that the slow-drift velocity of the structure is small compared to the phase velocity of the ambient waves. This approximation allows the formulation and solution of the linear and second-order free surface problems governing the slow-drift oscillation problem in the frequency domain, independently of the position of the structure. The magnitude of the corresponding wave forces in the time domain may then be obtained from the summation of the respective linear and quadratic time series.

Considerable effort has therefore been devoted to the theoretical study of the interaction of linear surface waves with three-dimensional structures undergoing a flow forward translation. Huijsmans & Hermans (1985) considered the forward motion of a ship and carried out a perturbation expansion of the forward-speed free-surface problem for small values of the parameter $\tau = \omega U/g$, where ω is the wave frequency and g the gravitational acceleration. The zero-speed problem was solved with a standard panel method using the wave source potential as the Green function.

The leading-order forward-speed problem was then treated by the derivation of an explicit surface Green function correct to $O(\tau)$. This approach was further pursued by Wu & Eatock Taylor (1990) in two dimensions and by Nossen, Grue & Palm (1991) for three-dimensional offshore structures. The latter study suggests the evaluation of the wave-drift coefficient in regular waves from a momentum conservation principle, which enjoys the computational benefits of analogous expressions for the drift forces in the zero-speed problem.

Zhao & Faltinsen (1988, 1989) considered the direct enforcement of the forward-speed free-surface condition by employing a Rankine panel method. This approach allows the inclusion of forward-speed effects of $O(\tau^2)$ which may become important when a strong current is present. The relative importance of forward-speed effects of $O(\tau)$ and $O(\tau^2)$ was investigated by Hermans (1991) for a vertical circular cylinder advancing in short waves. A ray theory was developed including all forward-speed effects and computations were carried out of the mean horizontal force. They suggest that effects of $O(\tau)$ may offer a good approximation of forward-speed effects even for values of τ which are not small.

In practice, the slow-drift oscillations of offshore structures occur in random short-crested waves. Current slow-drift oscillation models are based on the evaluation of the steady-state drift forces and wave-drift damping coefficients in monochromatic waves coupled with Newman's approximation for narrowband unidirectional wave spectra. When the wave energy is broadly distributed over the frequency axis and angular direction, important second-order wave effects contribute to the magnitude of the slow-drift excitation and wave-drift damping coefficients. The formulation of all linear and second-order free-surface problems governing the slow-drift excitation and damping forces is carried out in §2, under the assumption of a small slow-drift velocity and wave steepness. The solution of the second-order 'difference-frequency' problem for the slow-drift excitation force, has been considered in a number of studies (Faltinsen 1990), however, the corresponding problem governing the slow-drift damping has not yet been considered for three-dimensional structures. In broadband wave spectra, the solution of these second-order problems is expected to contribute significantly to the respective forces, yet the associated computational effort may be formidable. Therefore, accurate and efficient solutions for simplified geometries like arrays of vertical cylinders, would be valuable in practice and would also serve as benchmarks for future computations for bodies of arbitrary geometry.

An ordinary differential equation governing the rectilinear slow-drift oscillation of a body in the time domain is derived in §2.2. The assumption of a small value of τ leads to an important simplification. It allows the *a priori* evaluation of the slow-drift excitation and wave-drift damping quadratic transfer matrices in the frequency domain, independently of the slow-drift offset of the structure. Important viscous and nonlinear restoring effects may be added to the slow-drift equation without affecting this property.

In §3 the solution of the free-surface problem governing the diagonal terms of the wave-drift damping transfer matrix is considered. The mathematical geometry of a single vertical circular cylinder of infinite draught is considered first. The solution of the zero-speed diffraction problem is given by the classical McCamy and Fuchs solution. An analogous closed-form solution is derived in §3.1 for the leading forward-speed problem by combining the method of separation of variables with the use of the Weber transform.

The study of arrays of vertical circular cylinders is considerably more interesting in applications owing to their resemblance to the geometry of semi-submersible and

tension-leg offshore platforms. Linton & Evans (1990) derived an elegant extension of the zero-speed McCamy and Fuchs single-cylinder solution to an arbitrary spacing of vertical cylinders. Their method is extended in §3.2 to the solution of the leading-order forward-speed problem and is combined with the techniques used for the case of a single cylinder. In §4 an expression is derived for the wave-drift damping coefficient based on the momentum conservation principle. It requires the use of only the far-field wavelike form of the free-surface disturbance and its properties are analogous to the corresponding expression for the zero-speed horizontal drift forces and yaw moment. In §5 this expression is employed for the evaluation of the drift damping coefficient of a rectangular configuration of vertical circular cylinders corresponding to the geometry of a realistic offshore structure advancing in regular waves.

In monochromatic waves, the mean horizontal drift force and drift damping coefficients may be combined to estimate the mean drifting velocity of an unconstrained floating body. Such an expression is derived in §6, under the assumption that the drifting velocity is small. Employing the drift force and damping coefficients computed for the vertical cylinders it was found that a negative mean drifting velocity is possible for cylinder arrays but not for a single cylinder.

2. Mathematical formulation

Consider the interaction of gravity waves with a floating body undergoing a rectilinear slow-drift oscillation with velocity $U(t)$ along the positive X-axis of an inertial coordinate system (X, Y, Z), with X, Y on the calm free surface and the Z-axis pointing upwards. A coordinate system fixed on the body is related to the inertial system by the transformation $(x, y, z) = (X - X_0(t), Y, Z)$, where $U(t) = \mathrm{d}X_0/\mathrm{d}t$. Assume irrotational flow and introduce a velocity potential $\boldsymbol{\Phi}(\boldsymbol{X}, t)$ satisfying the Laplace equation and the nonlinear free-surface condition:

$$\frac{\mathrm{d}^2\boldsymbol{\Phi}}{\mathrm{d}t^2} + g\boldsymbol{\Phi}_z + 2\boldsymbol{\nabla}\boldsymbol{\Phi}\cdot\frac{\mathrm{d}\boldsymbol{\nabla}\boldsymbol{\Phi}}{\mathrm{d}t} + \tfrac{1}{2}\boldsymbol{\nabla}\boldsymbol{\Phi}\cdot\boldsymbol{\nabla}(\boldsymbol{\nabla}\boldsymbol{\Phi}\cdot\boldsymbol{\nabla}\boldsymbol{\Phi}) = 0 \tag{1}$$

enforced on the exact position of the free surface $z = \zeta(X, Y, t)$ defined by

$$\zeta = -\frac{1}{g}\left(\frac{\mathrm{d}\boldsymbol{\Phi}}{\mathrm{d}t} + \tfrac{1}{2}\boldsymbol{\nabla}\boldsymbol{\Phi}\cdot\boldsymbol{\nabla}\boldsymbol{\Phi}\right)_{z=\zeta}, \tag{2}$$

where g is the acceleration due to gravity and all time derivatives are understood with respect to the inertial frame. The Laplace equation and free-surface condition (1)–(2) must be supplemented by a prescribed normal velocity at the instantaneous position on the body boundary:

$$\boldsymbol{n}\cdot\boldsymbol{\nabla}\boldsymbol{\Phi} = \boldsymbol{n}\cdot\boldsymbol{V}_{\mathrm{b}}, \tag{3}$$

where $\boldsymbol{n}$ is a unit normal vector pointing out of the fluid domain and $\boldsymbol{V}_{\mathrm{b}}$ is the velocity of the body boundary. Finally, the flow velocity must vanish as $Z \to \infty$. The hydrodynamic pressure in the fluid domain is supplied by the Bernoulli equation,

$$p = -\rho\left(\frac{\mathrm{d}\boldsymbol{\Phi}}{\mathrm{d}t} + \tfrac{1}{2}\boldsymbol{\nabla}\boldsymbol{\Phi}\cdot\boldsymbol{\nabla}\boldsymbol{\Phi} + gZ\right), \tag{4}$$

where ρ is the water density.

Let $\phi(x, y, z, t) = \boldsymbol{\Phi}(X, Y, Z, t)$ be the velocity potential with respect to the body-

fixed coordinates. Time derivatives between the two coordinate systems are related by the Galilean transformation

$$\frac{\mathrm{d}\Phi}{\mathrm{d}t} = \left[\frac{\partial}{\partial t} - U(t)\frac{\partial}{\partial x}\right]\phi. \tag{5}$$

The substitution of $\phi(\boldsymbol{x},t) = \Phi(\boldsymbol{X},t)$ and (5) in (1)–(3) allows us to express the boundary-value problem with respect to the body-fixed coordinates for arbitrary $U(t)$.

Two independently small parameters are introduced, the characteristic wave slope δ and the forward-speed parameter $\tau_0 = U\omega_0/g$, where ω_0 is a typical wave frequency of $O(1)$. Small values of τ_0 correspond to a velocity U small relative to the phase velocity g/ω_0 of the wave. The characteristic frequency of the slowly varying motion is an order of magnitude smaller than ω_0, and terms proportional to $\mathrm{d}U/\mathrm{d}t$ are therefore neglected in the following analysis.

Assume the existence of a perturbation series expansion for the velocity potential and the wave elevation,

$$\phi(x,t) = \underbrace{\phi_{01}(\boldsymbol{x},t)}_{O(\tau_0)} + \underbrace{\phi_{10}(\boldsymbol{x},t)}_{O(\delta)} + \underbrace{\phi_{11}(\boldsymbol{x},t)}_{O(\delta\tau_0)} + \underbrace{\phi_{20}(\boldsymbol{x},t)}_{O(\delta^2)} + \underbrace{\phi_{21}(\boldsymbol{x},t)}_{O(\delta^2\tau_0)} + \ldots, \tag{6}$$

$$\zeta(x,y,t) = \underbrace{\zeta_{10}(x,y,t)}_{O(\delta)} + \underbrace{\zeta_{11}(x,y,t)}_{O(\delta\tau_0)} + \underbrace{\zeta_{20}(x,y,t)}_{O(\delta^2)} + \underbrace{\zeta_{21}(x,y,t)}_{O(\delta^2\tau_0)} + \ldots. \tag{7}$$

The first index in the velocity potentials and wave elevations corresponds to δ and the second to τ_0. We assume that δ and τ_0 are independently small, and will neglect terms of order higher than $\delta^2\tau_0$. A Taylor expansion of the right-hand side of (2) about the $z = 0$ plane and substitution of (6) and (7) in both sides of the equation, leads to the following definition for the two first wave elevations ζ_{ij}:

$$\zeta_{10} = -\frac{1}{g}\left(\frac{\partial\phi_{10}}{\partial t}\right)_{z=0}, \tag{8}$$

$$\zeta_{11} = -\frac{1}{g}\left(\frac{\partial\phi_{11}}{\partial t} + \nabla\phi_{10}\cdot\nabla\phi_{01}\right)_{z=0}. \tag{9}$$

In these expressions the double-body flow potential ϕ_{01} includes the uniform stream component $-Ux$. A similar Taylor series expansion of the free-surface condition (1) combined with the Galilean transformation (5) and the wave elevations (8), (9) leads to a sequence of free-surface boundary conditions for the velocity potentials ϕ_{ij} applied on the $z = 0$ plane:

$$\frac{\partial\phi_{01}}{\partial z} = 0, \tag{10}$$

$$\frac{\partial^2\phi_{10}}{\partial t^2} + g\frac{\partial\phi_{10}}{\partial z} = 0, \tag{11}$$

$$\frac{\partial^2\phi_{11}}{\partial t^2} + g\frac{\partial\phi_{11}}{\partial z} = \frac{\partial\phi_{10}}{\partial t}\frac{\partial^2\phi_{01}}{\partial z^2} - 2\nabla\phi_{01}\cdot\frac{\partial\nabla\phi_{10}}{\partial t}, \tag{12}$$

$$\frac{\partial^2\phi_{20}}{\partial t^2} + g\frac{\partial\phi_{20}}{\partial z} = -\frac{\partial}{\partial t}(\nabla\phi_{10}\cdot\nabla\phi_{10}) + \frac{1}{g}\frac{\partial\phi_{10}}{\partial t}\frac{\partial}{\partial z}\left[\frac{\partial^2\phi_{10}}{\partial t^2} + g\frac{\partial\phi_{10}}{\partial z}\right], \tag{13}$$

$$\frac{\partial^2\phi_{21}}{\partial t^2}+g\frac{\partial\phi_{21}}{\partial z}=-\tfrac{1}{2}\nabla\phi_{01}\cdot\nabla(\nabla\phi_{10}\cdot\nabla\phi_{10})-\nabla\phi_{10}\cdot\nabla\left(\nabla\phi_{01}\cdot\nabla\phi_{10}-2U\frac{\partial\phi_{10}}{\partial x}\right)$$
$$-\frac{\partial}{\partial z}\left[\zeta_{10}\left(\frac{\partial^2\phi_{11}}{\partial t^2}+g\frac{\partial\phi_{11}}{\partial z}\right)+\zeta_{11}\left(\frac{\partial^2\phi_{10}}{\partial t^2}+g\frac{\partial\phi_{10}}{\partial z}\right)\right]-2\nabla\phi_{11}\cdot\frac{\partial}{\partial t}\nabla\phi_{10}$$
$$-2\nabla\phi_{10}\cdot\frac{\partial}{\partial t}\nabla\phi_{11}-2\nabla\phi_{01}\cdot\frac{\partial}{\partial t}\nabla\phi_{20}-2\zeta_{10}\frac{\partial}{\partial z}\left(\nabla\phi_{10}\cdot\frac{\partial}{\partial t}\nabla\phi_{10}\right). \tag{14}$$

The double-body potential ϕ_{01} is the leading-order approximation for the steady flow for small τ_0; ϕ_{10} and ϕ_{11} are linear in δ and represent the zero-speed potential and its leading forward-speed correction, respectively. In order to compute the hydrodynamic force and responses of the body consistently to $O(\delta^2\tau_0)$, we also need to solve for ϕ_{20} and ϕ_{21}, which are the second-order equivalents of ϕ_{10} and ϕ_{11}.

The free-surface conditions (10)–(14) must be supplemented by a corresponding sequence of boundary conditions satisfied by the velocity potentials ϕ_{ij} on the body boundary. In this study the body will be assumed fixed relative to the translating frame, therefore all body-boundary conditions take the form

$$\frac{\partial\phi_{ij}}{\partial n}=0 \tag{15}$$

on the body wetted surface.

2.1. *The hydrodynamic forces*

From Bernoulli's equation and the expansion (6) for $\phi(\boldsymbol{x},t)$, it follows that the pressure in the fluid domain may be expanded in the form

$$p(\boldsymbol{x},t)=\underbrace{p_{00}(\boldsymbol{x})}_{O(1)}+\underbrace{p_{01}(\boldsymbol{x},t)}_{O(\tau_0)}+\underbrace{p_{10}(\boldsymbol{x},t)}_{O(\delta)}+\underbrace{p_{11}(\boldsymbol{x},t)}_{O(\delta\tau_0)}+\underbrace{p_{20}(\boldsymbol{x},t)}_{O(\delta^2)}+\underbrace{p_{21}(\boldsymbol{x},t)}_{O(\delta^2\tau_0)}+\ldots, \tag{16}$$

where p_{00} is the hydrostatic, p_{10} the linear pressure, and p_{01} the pressure due to the double body flow. The remaining components are defined by the relations

$$p_{11}=-\rho\left[\frac{\partial\phi_{11}}{\partial t}+\nabla\phi_{10}\cdot\nabla\phi_{01}\right], \tag{17}$$

$$p_{20}=-\rho\left[\frac{\partial\phi_{20}}{\partial t}+\tfrac{1}{2}\nabla\phi_{10}\cdot\nabla\phi_{10}\right], \tag{18}$$

$$p_{21}=-\rho\left[\frac{\partial\phi_{21}}{\partial t}+\nabla\phi_{01}\cdot\nabla\phi_{20}+\nabla\phi_{11}\cdot\nabla\phi_{10}\right]. \tag{19}$$

The hydrodynamic force experienced by the body may be obtained by integration of p_{ij} over its wetted surface or by the appropriate enforcement of the momentum conservation principle. It follows that the corresponding expansion of the force on the body becomes

$$\boldsymbol{F}(t)=\underbrace{\boldsymbol{F}_{10}(t)}_{O(\delta)}+\underbrace{\boldsymbol{F}_{11}(t)}_{O(\delta\tau_0)}+\underbrace{\boldsymbol{F}_{20}(t)}_{O(\delta^2)}+\underbrace{\boldsymbol{F}_{21}(t)}_{O(\delta^2\tau_0)}+\ldots. \tag{20}$$

Pressure integration yields the definitions

$$\boldsymbol{F}_{1i}(t)=\iint_S p_{1i}(t)\,\boldsymbol{n}\,\mathrm{d}s, \tag{21}$$

$$\boldsymbol{F}_{20}(t)=\iint_S p_{20}(t)\,\boldsymbol{n}\,\mathrm{d}s+\tfrac{1}{2}\rho g\int_{\mathrm{WL}}\zeta_{10}^2(t)\,\boldsymbol{n}\,\mathrm{d}l, \tag{22}$$

$$\boldsymbol{F}_{21}(t)=\iint_S p_{21}(t)\,\boldsymbol{n}\,\mathrm{d}s+\rho g\int_{\mathrm{WL}}\zeta_{10}(t)\,\zeta_{11}(t)\,\boldsymbol{n}\,\mathrm{d}l, \tag{23}$$

where the hydrodynamic pressure and wave elevation components have been defined above. $\bar{S}$ and WL are the mean wetted body surface and its intersection with $z = 0$, respectively.

In undirectional random gravity waves obeying the Gaussian model, the linear and second-order forces assume the following representations:

$$F_{1i}(t, X) = \mathrm{Re} \sum_k A_k \mathscr{F}_{1i}(\omega_k) \exp\left[\mathrm{i}\omega_k t - \mathrm{i}\nu_k X(t)\right], \tag{24}$$

$$F_{2i}(t, X) = \mathrm{Re} \sum_k \sum_l A_k A_l^* \mathscr{F}_{2i}(\omega_k, \omega_l) \exp\left[\mathrm{i}(\omega_k - \omega_l)t - \mathrm{i}(\nu_k - \nu_l) X(t)\right], \tag{25}$$

where $i = 0, 1$ for the zero and forward-speed components respectively, $\nu_k = \omega_k^2/g$ and the summations are over arrays of discrete wave frequencies. The complex wave amplitudes A_k have a random phase uniformly distributed in $(-\pi, \pi)$ and a modulus defined by the ambient wave spectrum. The complex force transfer functions $\mathscr{F}$ are obtained from the solution in the frequency domain of the boundary-value problems for ϕ_{ij} formulated in this section. Expressions (24) and (25) also account for the phase variation of the linear and second-order forces due to the offset $X(t)$ of the structure from its mean position.

The second-order force defined by (25) includes only the 'difference-frequency' component which is responsible for the slow-drift oscillations of floating structures. The corresponding 'sum-frequency' component is omitted since it contains little energy in the frequency range where slow-drift oscillation occur.

2.2. *A model slow-drift equation of motion*

Consider the case of a body undergoing a rectilinear slow-drift oscillation excited by ambient waves and restrained by a linear restoring mechanism. Including only ideal fluid effects and assuming for simplicity that the body is fixed at its mean translating position, we obtain from Newton's law

$$(M + A)\frac{\mathrm{d}^2 X_0(t)}{\mathrm{d}t^2} + CX_0(t) = F_{20}(t, X) + F_{21}(t, X), \tag{26}$$

where M is the body mass, A its added mass in the direction of translation obtained from the solution of the double-body flow and C is a linear restoring coefficient. By definition, the second-order force F_{21} depends linearly on τ_0 therefore we may set $F_{21} = -\dot{X}_0(t) B(t, X)$ and reduce the slow-drift equation of motion to the form

$$(M + A)\frac{\mathrm{d}^2 X_0(t)}{\mathrm{d}t^2} + B(t, X)\frac{\mathrm{d}X_0(t)}{\mathrm{d}t} + CX_0(t) = F_{20}(t, X). \tag{27}$$

The force coefficients $B(t, X)$, $F_{20}(t, X)$ are known as the slow-drift 'damping' and 'excitation' mechanisms supplied by the ambient random waves. Both are second-order quantities accepting representations analogous to (25), therefore the wave-drift damping force coefficient may be cast in the form

$$B(t; X) = \mathrm{Re} \sum_k \sum_l A_k A_l^* \mathscr{B}(\omega_k, \omega_l) \exp\left[\mathrm{i}(\omega_k - \omega_l)t - \mathrm{i}(\nu_k - \nu_l) X(t)\right]. \tag{28}$$

The computational effort necessary for the evaluation of the quadratic transfer matrices $\mathscr{F}_{20}(\omega_k, \omega_l)$, $\mathscr{B}(\omega_k, \omega_l)$ for three-dimensional geometries would be formidable. Therefore, Newman's approximation for narrowbanded wave spectra is widely used.

According to this approximation the slow-drift excitation force and damping coefficients may be approximated in terms of the diagonal elements of the corresponding quadratic transfer matrices, $\mathscr{F}_{20}(\omega_k, \omega_l)$ and $\mathscr{B}(\omega_k, \omega_l)$. The computation of the off-diagonal elements of $\mathscr{F}_{20}$ has been considered in a number of studies (Faltinsen 1990), yet no study has yet attempted the evaluation of the off-diagonal elements of the drift-damping quadratic transfer matrix $\mathscr{B}$ for three-dimensional bodies.

In particular, $\mathscr{F}_{20}(\omega, \omega)$ is the steady-state drift force exerted upon the body by a unit-amplitude regular wave of frequency ω and may be obtained in terms of the linear velocity potential ϕ_{10}. The corresponding quantity $\mathscr{B}(\omega, \omega)$ is known as the wave-drift damping coefficient and represents the leading-order forward speed correction to the drift force in regular waves. It may be determined in terms of the linear velocity potentials ϕ_{10}, ϕ_{11}, the solution of the double-body flow ϕ_{01} and of the second-order potential ϕ_{20} at the zero value of the difference frequency. The complete definition of the slow-drift excitation and damping forces requires the evaluation of the second-order potentials ϕ_{20} and ϕ_{21} for finite values of the difference frequency, as may be inferred from the corresponding pressure components p_{20} and p_{21} defined by (18) and (19), respectively.

The present study concentrates upon the evaluation of the wave-drift damping coefficient $\mathscr{B}(\omega, \omega)$ in the diffraction problem. An explicit solution will be derived for ϕ_{11}, and will be combined with a momentum conservation theorem to evaluate the wave-drift damping coefficients of a single and multiple vertical circular cylinders.

3. Explicit solution for ϕ_{11} for vertical circular cylinders

3.1. *A single cylinder*

In this section, explicit solutions will be derived for the velocity potential ϕ_{11} for circular cylindrical body geometries intersecting the free surface at right angles. This solution will be obtained in the frequency domain and will be used to derive expressions for the wave-drift damping coefficient $\mathscr{B}(\omega, \omega)$ for a single and multiple circular cylinders.

Consider a body with a vertical, circular cylindrical geometry of infinite draught advancing in the positive x-direction with velocity U. The body is assumed fixed at its mean translating position and is otherwise free to interact with ambient regular waves of absolute frequency ω_0 and direction β relative to the positive x-axis. The linearized wave disturbance governed by the velocity potentials ϕ_{10} and ϕ_{11} will be time harmonic, thus we may set

$$\phi_{10}(\boldsymbol{x}, t) = \mathrm{Re}\{\varphi(\boldsymbol{x})\, \mathrm{e}^{\mathrm{i}\omega t}\}, \tag{29}$$

$$\phi_{11}(\boldsymbol{x}, t) = \tau_0\, \mathrm{Re}\{\psi(\boldsymbol{x})\, \mathrm{e}^{\mathrm{i}\omega t}\}, \tag{30}$$

where the frequency of encounter is defined by $\omega = \omega_0 - \nu U \cos\beta$. Upon substitution in the free-surface conditions (11) and (12) and use of the relation $\partial/\partial t = \mathrm{i}\omega$, it follows that on $z = 0$

$$-\nu\varphi + \varphi_z = 0, \tag{31}$$

$$-\nu\psi + \psi_z = -2\mathrm{i}\nabla\bar{\Phi}\cdot\nabla\varphi - 2\nu\cos\beta\varphi, \tag{32}$$

where $\nu = \omega_0^2/g$. The second term in the inhomogeneous free-surface condition for the potential ψ accounts for forward-speed effects contained in the frequency of encounter ω. Earlier studies have elected to treat this effect by including it in the frequency of encounter at which the above boundary-value problems have been

solved. The present approach allows the complete decoupling of zero from forward-speed effects which is very desirable in the formulation and solution of the slow-drift equation of motion.

For the cylindrical bodies of infinite draught, there is no z-variation in the double-body flow, which is normalized as follows: $\phi_{01} = U\bar{\Phi}(x,y) = -U(x-\bar{\phi})$. For a single circular cylinder the disturbance potential $\bar{\phi}$ is that of a dipole:

$$\bar{\phi} = -\frac{a^2}{r}\cos\theta, \tag{33}$$

where $(x,y) = r(\cos\theta, \sin\theta)$. The condition of zero normal velocity for the double-body and diffraction potentials on the body surface S yields

$$\frac{\partial\bar{\Phi}}{\partial n} = \frac{\partial\varphi}{\partial n} = \frac{\partial\psi}{\partial n} = 0. \tag{34}$$

The determination of ψ can be decomposed into a sequence of problems. The leading-order forward-speed potential ψ is written as the sum of the individual potentials ψ_1, ψ_2 and ψ_3, subject to the following boundary conditions on $z = 0$ and on the circular boundary:

$$\left.\begin{aligned} -\nu\psi_1 + \psi_{1z} &= 2\mathrm{i}\varphi_x - 2\nu\cos\beta\varphi, \\ \psi_{1r} &= v(z); \end{aligned}\right\} \tag{35}$$

$$\left.\begin{aligned} -\nu\psi_2 + \psi_{2z} &= 0, \\ \psi_{2r} &= -v(z); \end{aligned}\right\} \tag{36}$$

$$\left.\begin{aligned} -\nu\psi_3 + \psi_{3z} &= -2\mathrm{i}\nabla\bar{\phi}\cdot\nabla\varphi, \\ \psi_{3r} &= 0. \end{aligned}\right\} \tag{37}$$

The solution to problem (35) may be obtained by inspection of the free-surface condition (31). The velocity potential

$$\psi_1(x,y,z) = 2\left(\mathrm{i}\frac{\partial}{\partial x} - \nu\cos\beta\right)\frac{\partial\varphi_D}{\partial\nu} \tag{38}$$

may be verified to satisfy the Laplace equation and the two equations in (35), here $v(z)$ is given by

$$v(z) = 2\left(\mathrm{i}\frac{\partial}{\partial x} - \nu\cos\beta\right)\frac{\partial^2\varphi_D}{\partial\nu\,\partial r}. \tag{39}$$

The zero-speed potential φ has been decomposed into the diffraction potential φ_D and the incident wave potential φ_I. The latter has been omitted from the solution for φ_1 since its contribution satisfies the homogeneous free surface condition in (35) and is therefore not a desired solution. The total zero-speed potential φ, known as the McCamy and Fuchs solution,

$$\varphi = \frac{igA}{\omega_0}e^{\nu z}\left(\exp\left[-\mathrm{i}\nu(x\cos\beta + y\sin\beta)\right] - \sum_m\left((-\mathrm{i})^m\frac{J'_m(\nu a)}{H^{(2)\prime}_m(\nu a)}H^{(2)}_m(\nu r)\exp\left[\mathrm{i}m(\theta-\beta)\right]\right)\right), \tag{40}$$

where J_m, $H^{(2)}_m$ are the Bessel and Hankel functions, respectively, and the summation is over all integers m.

The determination of ψ_2 and ψ_3 is simplified if only their far-field components are needed. This will be the case if conservation of momentum is used as in §4 in order

to evaluate the wave-drift damping coefficient. Therefore, the remainder of this section seeks to determine the wavelike components of the potentials ψ which are dominant in the far field.

The far-field wave component of the 'radiation' potential of ψ_2 admits the Fourier decomposition,

$$\psi_2 = \mathrm{e}^{\nu z} \sum_m \alpha_m H_m^{(2)}(\nu r)\, \mathrm{e}^{\mathrm{i}m\theta}. \tag{41}$$

The unknown complex coefficients α_m may be determined in terms of the velocity $v(z)$ induced by ψ_1 on the cylinder, by employing Havelock's wavemaker theory. The result is

$$\alpha_m = -\frac{2}{H_m^{(2)\prime}(\nu a)} \int_{-\infty}^{0} \mathrm{d}z\, v_m(z)\, \mathrm{e}^{\nu z}, \tag{42}$$

where $v(z) = \sum_m v_m(z)\, \mathrm{e}^{\mathrm{i}m\theta}$.

In order to solve (37) we first expand ψ_3 in the Fourier series

$$\psi_3 = \sum_m \psi_{3m}\, \mathrm{e}^{\mathrm{i}m\theta}, \tag{43}$$

and invoke the Weber transform pair for ψ_{3m} (Davies 1978),

$$\tilde{\psi}_{3m}(k) = \int_a^\infty r\, \mathrm{d}r\, \psi_{3m}(r)\, W_m(kr), \tag{44}$$

$$\psi_{3m}(r) = \int_0^\infty k\, \mathrm{d}k\, \tilde{\psi}_{3m}(k) \frac{W_m(kr)}{J'_m(ka)^2 + Y'_m(ka)^2}, \tag{45}$$

where

$$W_m(kr) = Y'_m(ka)\, J_m(kr) - J'_m(ka)\, Y_m(kr). \tag{46}$$

The Weber transform exists here due to the rapid decay of $\nabla\bar{\phi}$ as $r \to \infty$. This would not be the case with (35) because of the $1/r^{\frac{1}{2}}$ decay of the forcing term in the free-surface condition. The transformation of the Laplace equation, free-surface condition and the body boundary condition for ψ_3, leads to the following set of equations for $\tilde{\psi}_{3m}(k)$:

$$\left(\frac{\partial^2}{\partial z^2} - k^2\right) \tilde{\psi}_{3m} = 0, \tag{47}$$

$$\left(\frac{\partial}{\partial z} - \nu\right) \tilde{\psi}_{3m} = \tilde{F}_m(k), \tag{48}$$

$$\tilde{\psi}_{3mr} = 0, \tag{49}$$

where $\tilde{F}(k) = \sum_m \tilde{F}_m(k)\, \mathrm{e}^{\mathrm{i}m\theta}$ is the Weber transform of the right-hand side of the first equation in (37). The solution for ψ_{3m} follows upon substitution of the solution for $\tilde{\psi}_{3m}$ into (45),

$$\psi_{3m}(r) = \int_0^\infty \mathrm{d}k \frac{k}{k-\nu} \tilde{F}_m(k) \frac{W_m(kr)}{J'_m(ka)^2 + Y'_m(ka)^2} \mathrm{e}^{kz} \tag{50}$$

with the path integration intended above the pole at $k = \nu$. The identity

$$\frac{W_m(kr)}{J'_m(ka)^2 + Y'_m(ka)^2} = -\frac{1}{2\mathrm{i}} \left(\frac{H_m^{(1)}(kr)}{H_m^{(1)\prime}(ka)} - \frac{H_m^{(2)}(kr)}{H_m^{(2)\prime}(ka)} \right) \tag{51}$$

allows the deformation of the contour of integration in the upper/lower k-plane for

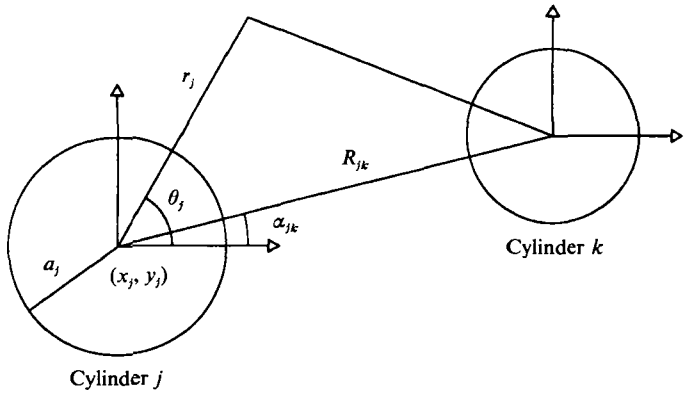

FIGURE 1. Definition of parameters for an array of cylinders.

the first/second terms in (51). As $r \to \infty$, the wavelike contribution to ψ_{3m} arises from the residue at $k = \nu$, and takes the form

$$\psi_3 = -\pi\nu\, e^{\nu z} \sum_m \frac{\tilde{F}_m(\nu)}{H_m^{(2)\prime}(\nu a)} H_m^{(2)}(\nu r)\, e^{im\theta}, \tag{52}$$

which represents outgoing waves satisfying the homogeneous free-surface condition. The far-field wavelike solutions for ψ_2 and ψ_3 given by (41) and (52) will later be combined with ψ_1 defined by (38) in order to evaluate the wave-drift damping using a momentum conservation principle.

The determination of the second-order potential ϕ_{20} at zero difference frequency is not necessary when the wave drift damping is determined from a far-field momentum conservation method. In the diffraction problem studied here, this value of ϕ_{20} may actually be shown to be zero. This follows from the vanishing of the forcing term in the second-order free-surface condition (13) due to the exponential decay with depth of the zero-speed diffraction potential around a vertical cylinder.

3.2. *Arrays of vertical cylinders*

Several floating structures encountered in practice consist of vertical circular legs piercing the free surface. Therefore, the extension of the results for the single cylinder to arrays of cylinders would be valuable in applications.

An elegant extension of the McCamy and Fuchs solution to an array of N arbitrarily spaced circular cylinders was derived by Linton & Evans (1990). The total diffraction velocity potential in the vicinity of cylinder j was expressed in the form

$$\varphi^j = \frac{igA}{\omega_0} e^{\nu z} \sum_m A_m^j [Z_m^j H_m^{(2)}(\nu r_j) - J_m(\nu r_j)]\, e^{im\theta_j}, \tag{53}$$

where (r_j, θ_j) are the local radial and angular coordinates centred at the jth cylinder, as shown in figure 1 and $Z_m^j = J_m'(\nu a_j)/H_m^{(2)\prime}(\nu a_j)$. The complex coefficients A_m^j account for the hydrodynamic interaction between the cylinders and are determined from the solution of a linear system of equations obtained from the enforcement of the boundary condition on each cylinder:

$$A_m^k + \sum_{\substack{j=1 \\ *k}}^{N} \sum_{n=-M}^{M} A_n^j Z_n^j \exp[i(n-m)\alpha_{jk}] H_{n-m}^{(2)}(\nu R_{jk}) = -I_k \exp[-im(\pi/2+\beta)],$$

$$k = 1, \ldots, N, \quad m = -M, \ldots, M \tag{54}$$

where $I_k = \exp[-i\nu(x_k \cos\beta + y_k \sin\beta)]$ is the phase factor associated with cylinder k. The geometrical parameters α_{jk}, R_{jk} and (x_k, y_k) are defined in figure 1. The infinite series corresponding to that in (53) has been truncated to $(2M+1)$ terms.

The exact double-body velocity potential $\bar{\Phi}$ for an array of cylinders corresponds to a uniform flow past an array of circles in two dimensions. For the cylinder spacing encountered in practice, we may however ignore hydrodynamic interactions in $\bar{\Phi}$, due to the rapid decay with r_j of the quantity $\nabla\bar{\Phi}$ which enters the definition of the forward speed potential (32). Therefore, the steady velocity potential $\bar{\Phi}$ in the vicinity of cylinder j is expressed as the sum of a uniform flow $-x$ and the disturbance potential $\bar{\phi}^j$ due to a dipole, defined by

$$\bar{\phi}^j = -\frac{a_j^2}{r_j}\cos\theta_j. \tag{55}$$

The forward-speed potentials ψ_i, $(i = 1, 2, 3)$ are again subject to (35)–(37) and (39). Here, φ, φ_D and $\bar{\phi}$ are replaced by φ^j, $\varphi^j - \varphi_I^j$ and $\bar{\phi}^j$, respectively, where φ_I^j is the incident wave potential expressed in terms of the local coordinates on cylinder j and the phase factor I_j. The solution around each cylinder j may therefore be obtained by employing the method presented in §3.1 combined with an extension of the Linton–Evans interaction theory, which is derived next.

The potential ψ_1 around each cylinder may be determined easily by employing the coordinates on cylinder j and using the explicit relation (38). The ν-derivative of φ^j gives rise to a new set of coefficients, $B_m^j \equiv (\partial/\partial\nu)A_m^j$. They have been determined by taking the ν-derivative of (54) and solving the resulting linear system of equations for B_m^j. An alternative approach would involve the use of numerical differentiation of the ν-dependence of the coefficients A_m^j.

The determination of the wavelike components of ψ_2 and ψ_3 requires the determination of new sets of interaction coefficients, which will be discussed next. Consider the generalized radiation velocity potential χ, subject to the Laplace equation and the boundary conditions on $z = 0$ and on each cylinder j, respectively,

$$-\nu\chi + \chi_z = 0, \tag{56}$$

$$\chi_r = u^j(z), \tag{57}$$

where $u^j(z)$ admits the Fourier decomposition

$$u^j(z) = \sum_m u_m^j(z)\, e^{im\theta_j}. \tag{58}$$

The solution of this boundary-value problem will next be carried out by extending the Linton–Evans interaction theory to the radiation problem. Only wavelike interactions between the cylinders will be accounted for, while interactions arising from the non-wavelike component of the radiation solution around each cylinder will be omitted.

The potential χ may be decomposed into two components. The first component is the sum of wave disturbances 'radiated' from single cylinders acting as wavemakers, and is subject to the boundary condition (57) on cylinder j. This component is free of interaction effects and around cylinder j is defined by

$$\chi_0^j = \sum_m \beta_m^j H_m^{(2)}(\nu r_j)\exp[im\theta_j + \nu z], \tag{59}$$

where

$$\beta_m^j = \frac{2}{H_m^{(2)\prime}(\nu a_j)}\int_{-\infty}^{0} u_m^j(z)\, e^{\nu z}\, dz. \tag{60}$$

The second component consists of the 'diffracted' wave disturbance around cylinder j due to the waves 'radiated' by the other cylinders and may be expressed in the form

$$\chi_1^j = \sum_m C_m^j Z_m^j H_m^{(2)}(\nu r_j) \exp[im\theta_j + \nu z], \tag{61}$$

where C_m^j are unknown interaction coefficients and the complex constants Z_m^j have been defined in (53).

The total potential χ, may therefore be written as the sum of all radiated and diffracted wave disturbances, or

$$\chi = \sum_{j=1}^{N} (\chi_0^j + \chi_1^j). \tag{62}$$

The unknown interaction coefficients C_m^j may be determined by enforcing a homogeneous boundary condition on each cylinder for the velocity potential χ_1. Expressing χ_1 in terms of the coordinates of cylinder j requires the use of Graf's addition theorem for Bessel functions (Abramowitz & Stegun 1972, eqn. 9.1.79). Algebra analogous to that in Linton & Evans leads to the following system of equations for the coefficients C_m^k:

$$C_m^k + \underbrace{\sum_{j=1}^{N} \sum_{n=-M}^{M}}_{+k} (C_n^j Z_n^j + \beta_n^j) \exp[i(n-m)\alpha_{jk}] H_{n-m}^{(2)}(\nu R_{jk}) = 0,$$
$$k = 1, \ldots, N, \quad m = -M, \ldots, M. \tag{63}$$

Following the determination of the 'radiation' interaction coefficients C_m^j, Graf's addition theorem and equation (63) allow the total potential χ around cylinder j to be expressed in the form

$$\chi^j = \sum_m [(C_m^j Z_m^j + \beta_m^j) H_m^{(2)}(\nu r_j) - C_m^j J_m(\nu r_j)] \exp[im\theta_j + \nu z]. \tag{64}$$

In the special case $w^j(z) = \cos\theta_j$, equation (64) supplies the solution to the surge radiation problem of an array of vertical cylinders. The performance of this interaction theory which omits non-wavelike interactions between the cylinders is illustrated in figure 2. A square configuration of four cylinders corresponding to a realistic structure was considered with radii equal to $\frac{1}{4}$ of their spacing. The surge added mass was determined using the interaction theory and was compared with exact computations using the three-dimensional panel method WAMIT. The agreement is very satisfactory and consistent with earlier interaction theories based on the same approximation.

The solution for the forward-speed potential ψ_2 now follows easily from the derivation of χ, by setting $w^j(z) = -v^j(z)$ with $v^j(z)$ given from the r-derivative of the solution for ψ_1 presented in this Section.

The remaining potential ψ_3 may be determined along similar lines as ψ_2. It will also consist of a 'radiated' and a 'diffracted' component. The former may be determined as for the single cylinder by making use of the Weber transform. The governing equation and boundary conditions are given by (47)–(49). For cylinder j, the right-hand side of (48) takes the form

$$\tilde{F}_m^j(k) = -2i \int_a^\infty r_j \, dr_j \, \lambda_m(r_j) \, W_m^j(kr_j), \tag{65}$$

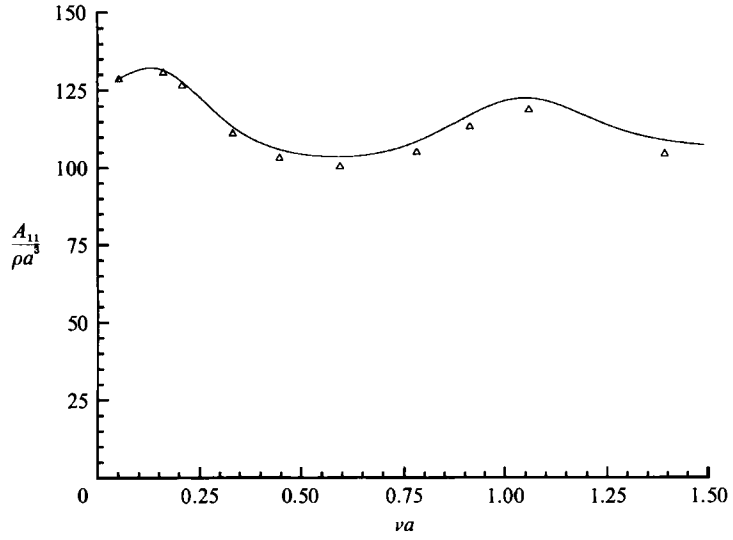

FIGURE 2. Added mass (solid line) for an array of four cylinders, with spacing 4 times the cylinder radius. The triangles represent the same quantities obtained by WAMIT. The analytic results do not include the interaction of evanescent modes. $\nu = \omega_0^2/g$ is the wavenumber for infinite water depth and a is the cylinder radius.

where
$$\nabla\bar{\phi}^j \cdot \nabla\varphi^j = \sum_m \lambda_m(r_j)\, e^{im\theta_j}, \tag{66}$$

$$W_m^j(kr_j) = Y'_m(ka_j)\, J_m(kr_j) - J'_m(ka_j)\, Y_m(kr_j). \tag{67}$$

The double-body velocity potential $\bar{\phi}^j$ is defined by (55) and the zero-speed diffraction solution φ^j is obtained from the Linton & Evans solution.

The 'radiated' wavelike component of ψ_3 arises from the residue of the integral; (50) and takes the form suggested by (52). On the surface of cylinder j it satisfies the boundary condition

$$\psi_{3r} = -\pi\nu^2 e^{\nu z} \sum_m \tilde{F}_m^j(\nu)\, e^{im\theta_j}, \tag{68}$$

and on $z = 0$ it is subject to the homogeneous free-surface condition. It follows that the wavelike component of ψ_3 may be determined by employing the interaction theory derived in the present section for the generalized radiation potential χ. For ψ_3, the normal velocity to be enforced on cylinder j is given by $u^j(z) = \psi_{3r}$.

4. The wave-drift damping coefficient

The second-order difference-frequency wave force experienced by a floating body in polychromatic waves has been defined by the double series (25) of §2.1. This article is concerned with the evaluation of the diagonal terms of the quadratic transfer matrix $\mathscr{F}_{2i}(\omega_k, \omega_l)$, obtained by setting $\omega_k = \omega_l = \omega$. It follows from (25) that the corresponding terms in the series supply the mean value of the second-order force, defined as follows

$$\bar{F}_{2i}(t) = \sum_k |A_k|^2 \,\mathrm{Re}\,[\mathscr{F}_{2i}(\omega_k, \omega_k)]. \tag{69}$$

In monochromatic waves of frequency ω_0 only one term survives in the series (69). For $i = 0$, it represents the mean drift force experienced by a stationary body, while

with $i = 1$ it denotes the leading-order forward-speed correction to the drift force when the body advances slowly in the positive $x-$direction. In regular waves we may therefore set, with an error of $O(\tau_0^2)$,

$$\bar{F}_2(t) = |A|^2 \operatorname{Re}[\mathscr{F}_{20}(\omega_0) + \mathscr{F}_{21}(\omega_0)] = D(\omega_0) - UB(\omega_0), \tag{70}$$

where U is the velocity of the body, $D(\omega_0)$ is the drift force and $B(\omega_0)$ the drift damping coefficient. From the momentum conservation principle we may express the x-component of the drift force on the body as an integral over a control surface S_∞, which extends from the sea bottom up to the free surface and is fixed at some distance away from the translating position of the body. The drift force, correct to $O(A^2)$ for an arbitrary velocity U, may be written as follows (Nossen *et al.* 1991):

$$F_x = \rho \int_{\bar{S}_\infty} \overline{[\phi_x \phi_n - \tfrac{1}{2}\nabla\phi\cdot\nabla\phi n_1]}^{\mathrm{t}}\, \mathrm{d}S + \frac{\rho}{2g}\int_{c_\infty} \overline{[(\phi_t)^2 - U^2(\phi_x)^2]}^{\mathrm{t}}\, n_1\, \mathrm{d}l, \tag{71}$$

where $\bar{S}_\infty$ is the control surface below $z = 0.$ and c_∞ is its intersection with $z = 0$. The subscripts x, n and t indicate the partial derivatives with respect to the respective variables. Using expansion (6), equation (29) and (30) for ϕ in (71), and keeping terms linear in U, we obtain the following expression for the drift damping coefficient:

$$B(\omega_0) = -\frac{\rho\omega_0}{2g}\operatorname{Re}\left[\int_{\bar{S}_\infty} (\varphi_x \psi_n^* + \varphi_n \psi_x^* - \nabla\varphi\cdot\nabla\psi^* n_1)\, \mathrm{d}S + \nu\int_{c_\infty} (\varphi\psi^* - \cos\beta|\varphi|^2)\, n_1\, \mathrm{d}l\right]. \tag{72}$$

The analogous familiar definition of the drift force $D(\omega_0)$ is

$$D(\omega_0) = \tfrac{1}{2}\rho \operatorname{Re}\left[\int_{\bar{S}_\infty} (\varphi_x \varphi_n^* - \tfrac{1}{2}\nabla\varphi\cdot\nabla\varphi^* n_1)\, \mathrm{d}S + \nu\int_{c_\infty} \tfrac{1}{2}|\varphi|^2 n_1\, \mathrm{d}l\right]. \tag{73}$$

For the single cylinder the complex velocity potentials to be used in (72) and (73) are given by

$$\varphi = \frac{\mathrm{i}gA}{\omega_0}\mathrm{e}^{\nu z}\sum_m (-\mathrm{i})^m \left[J_m(\nu r) - \frac{J_m'(\nu a)}{H_m^{(2)\prime}(\nu a)} H_m^{(2)}(\nu r)\right]\mathrm{e}^{\mathrm{i}m(\theta-\beta)}, \tag{74}$$

$$\psi = 2\left[\mathrm{i}\frac{\partial}{\partial x} - \nu\cos\beta\right]\frac{\partial\varphi}{\partial\nu} + \mathrm{e}^{\nu z}\sum_m \left[\alpha_m - \pi\nu\frac{\tilde{F}_m(\nu)}{H_m^{(2)\prime}(\nu a)}\right] H_m^{(2)}(\nu r)\,\mathrm{e}^{\mathrm{i}m\theta}, \tag{75}$$

where $\alpha_m, \tilde{F}_m(\nu)$ are defined in §3.1.

For an array of cylinders, φ is given by (53). The wavelike component of the forward-speed potential ψ has been derived in §3.2. The non-wavelike disturbance decays rapidly at large distances from the cylinders and does not contribute to the wave-drift damping coefficient.

Expression (72) extends the corresponding far-field expression for the zero-speed drift forces which have been found to be more attractive in numerical computations relative to the near-field pressure integration method. For bodies of arbitrary shape, the integration surface $\bar{S}_\infty$ may be removed to infinity and the drift forces may be obtained as simple azimuthal integrations of the Kochin functions, known as the Maruo–Newman expressions (see Maruo 1960; Newman 1967). An extension of these results to the wave-drift damping force have been derived in Nossen *et al.* (1991) for bodies of general shape.

In the present study an alternative approach will be followed based on the derivation of a mathematical conservation theorem for the wave-drift damping coefficient defined by (72).

4.1. *Conservation law for the drift damping coefficient*

Expression (72) will be shown to be in conservation form, i.e. its value does not depend on the position of the control surface S_∞. This will be shown to be the case for two arbitrary velocity potentials φ and ψ subject to the free-surface conditions

$$\varphi_z - \nu\varphi = 0, \tag{76}$$

$$\psi_z - \nu\psi = 2\mathrm{i}\varphi_x - 2\nu\cos\beta\varphi. \tag{77}$$

Here it is important to note that all three wavelike components of ψ satisfy (77). In particular, ψ_1 is subject to (77) while ψ_2 and ψ_3, as defined by (41) and (52), satisfy the homogeneous form of (77).

We will use the following identity, valid for an arbitrary velocity potential ϕ over a closed surface S:

$$I(\phi) = \mathrm{Re}\iint_S \mathrm{d}S(\phi_x\phi_n - \tfrac{1}{2}\nabla\phi\cdot\nabla\phi n_1) = 0, \tag{78}$$

where n_1 is the x-component of the unit vector $\boldsymbol{n}$ normal to S and pointing out of the enclosed domain.

Apply now (78) to the potential $\phi = \varphi + \psi^*$ over the surface $S = S_{C_1} + S_{C_2} + S_F$, where S_{C_1} and S_{C_2} are two vertical, neighbouring surfaces and S_F is the annular strip on $z = 0$ between the intersecting contours C_1 and C_2. Assuming that the flow velocity vanishes at $z = -\infty$, (78) may be rewritten in the form

$$\mathrm{Re}\iint_{S_{C_1}+S_{C_2}+S_F} \mathrm{d}S(\varphi_x\psi_n^* + \varphi_n\psi_x^* - \nabla\varphi\cdot\nabla\psi^* n_1) = 0. \tag{79}$$

The integral over S_F, where $n_1 = 0$, can be simplified using the free-surface conditions (76) and (77). The integrand on this surface may be reduced to the form

$$\varphi_x\psi_z^* + \varphi_z\psi_x^* = \varphi_x(\nu\psi^* - 2\mathrm{i}\varphi_x^* - 2\nu\cos\beta\varphi^*) + \nu\varphi\psi_x^*. \tag{80}$$

Taking the complex conjugate of the last two terms in (80) and applying the identity $\mathrm{Re}\,(2\mathrm{i}\varphi_x\varphi_x^*) = 0$, it follows that

$$\begin{aligned}\mathrm{Re}\iint_{S_F} \mathrm{d}S(\varphi_x\psi_z^* + \varphi_z\psi_x^*) &= \mathrm{Re}\,\nu\iint_{S_F} \mathrm{d}S\frac{\partial}{\partial x}(\varphi\psi^* - \cos\beta\varphi\varphi^*) \\ &= \mathrm{Re}\oint_{C_1+C_2} \mathrm{d}l\,(\varphi\psi^* - \cos\beta\varphi\varphi^*)\,n_1,\end{aligned} \tag{81}$$

where Stokes' theorem has been used. A comparison of (72) with the identities (79) and (81) completes the proof of the conservation law for the drift damping coefficient.

The position of the control surface S_∞ in (72) may therefore be selected arbitrarily. It may for example be taken to coincide with the body surface, as long as only the wavelike components are included in the definition of the velocity potentials φ, ψ. All integrations suggested by (72) are carried out over the surface of each cylinder j by employing the explicit local wavelike solutions derived in §3.

5. Wave-drift damping computations

The method of conservation of momentum described in §4 has been used for the evaluation of the wave-drift damping coefficient for a single cylinder and an array of vertical cylinders of infinite draught.

The x-component of the slow-drift damping coefficient $B(\omega_0)$ for a single cylinder is illustrated in figure 3 as a function of νa, where $\nu = \omega_0^2/g$ is the wavenumber and

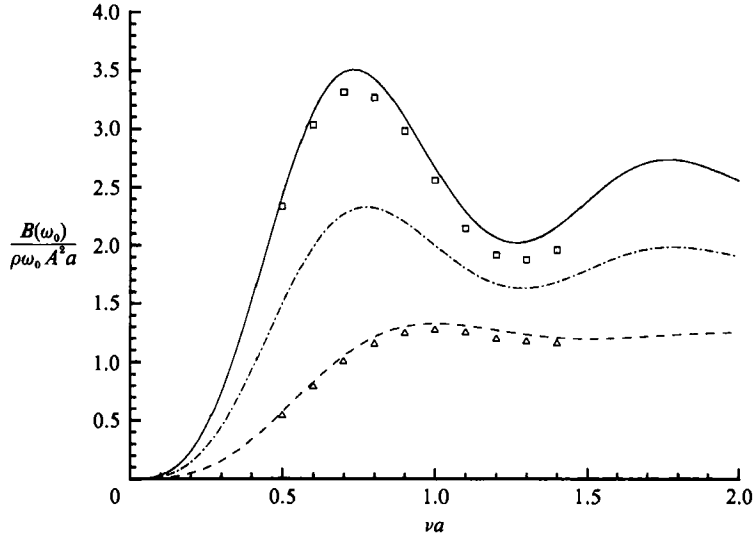

FIGURE 3. Slow drift damping coefficient for a single, vertical restrained cylinder. results are shown for different incident wave angles β relative to the positive x-axis: $\beta = 0$ (solid line), $\beta = 45°$ (dash-dotted line) and $\beta = 90°$ (dotted line). Comparison is made with Nossen *et al.* (1991) for $\beta = 0$ (squares) and $\beta = 90°$ (triangles).

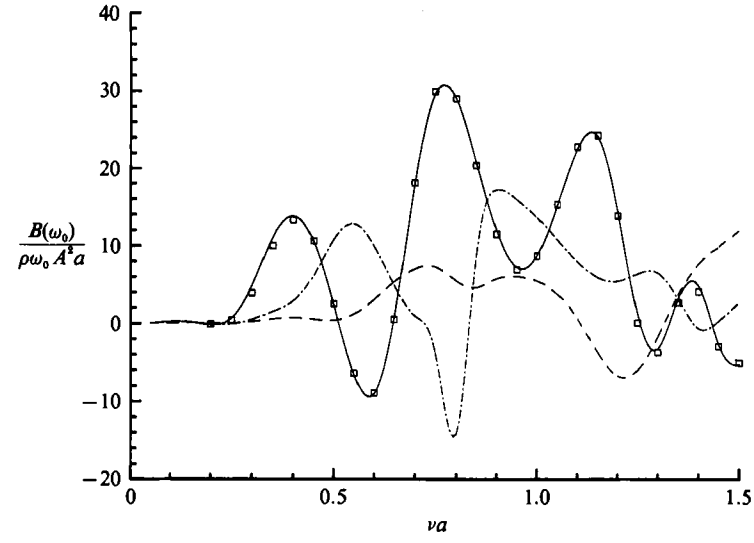

FIGURE 4. Same as figure 3 but for an array of four equal vertical, restrained cylinders. The cylinders are centred at the corners of a square with side-lengths 7 times the cylinder radius.

a the cylinder radius. The selected directions of the incident wave are $\beta = 0°$ (along the positive x-axis), $\beta = 45°$ and $\beta = 90°$ (along the positive y-axis). Comparison with the three-dimensional solution developed in Nossen *et al.* (1991) for bodies of general geometry is very satisfactory.

Figure 4 is equivalent to figure 3 for an array of four cylinders. Each cylinder is centred at the corner of a square with side-lengths equal to 7 times the radius of each cylinder. Comparison with independent computations of the wave-drift damping coefficient by the method of Nossen *et al.* (1991, private communication) for the same rectangular arrangement of cylinders is very gratifying over a wide range of

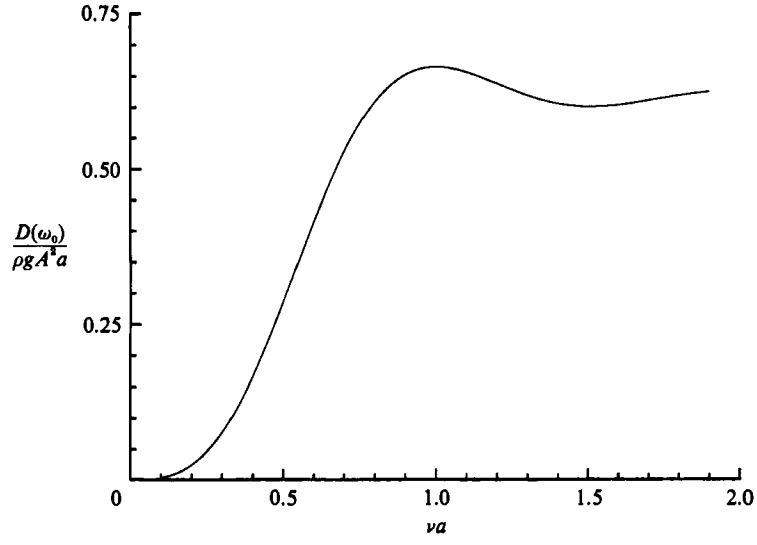

FIGURE 5. Drift force $D(\omega_0)$ for a single, vertical restrained cylinder. The incident wave is for $\beta = 0$.

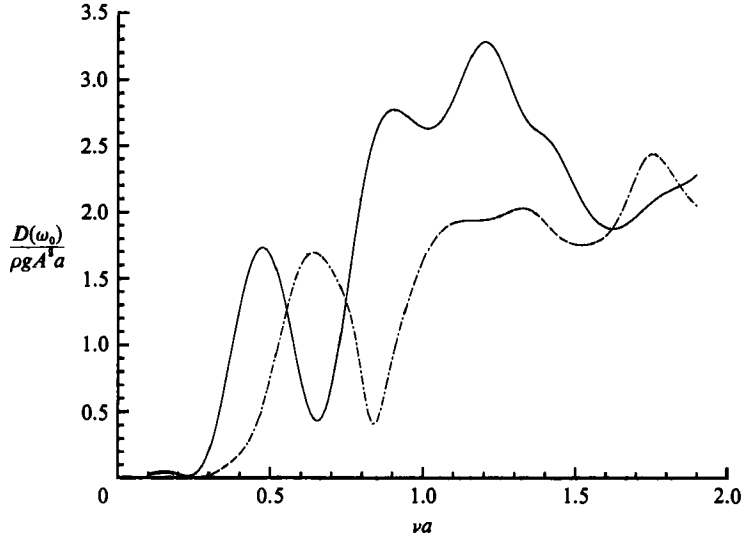

FIGURE 6. Drift force $D(\omega_0)$ for an array of four cylinders (see figure 4). The incident waves are for $\beta = 0$ (solid line) and $\beta = 45°$ (dash-dotted line).

frequencies. An important difference between the two sets of results is that the three-dimensional computations were carried out for truncated cylinders with draught equal to three radii. The remarkable agreement suggests that the wave-drift damping coefficient appears to be dominated by near-surface wave effects. Moreover it confirms the usefulness of the multiple-cylinder solution in applications. An accuracy of the order 10^{-5} was obtained for the array of cylinders by using $M \sim 10$ when solving for the interaction coefficients A_m^k and C_m^k.

Figures 5 and 6 illustrate the zero-speed force $D(\omega_0)$ for the same geometries and incident wave directions as figures 3 and 4, respectively. Strong wave interactions between the cylinders are evident for the array of four cylinders, as opposed to the

more smooth curves for the single cylinder. Such interaction effects are seen to lead to a negative drift damping coefficient for some wavelengths while the drift force remains positive for all frequencies. In particular, the negative drift damping seems to occur when the wavelength is approximately equal to the distance between cylinders in the direction of the propagation of the incident wave.

6. Drifting velocity of a body in regular waves

A body floating freely in regular waves will tend to drift in the direction of wave propagation. In steady state and for incident waves propagating along a plane of symmetry of the body, it will undergo a rectilinear drifting translation with mean velocity U. From Newton's law it follows that the mean force in the direction of translation must vanish. Therefore, it follows from (70) that to leading order for a small drifting velocity, U equals the ratio of the drift force to the drift damping coefficient,

$$U = \frac{D(\omega_0)}{B(\omega_0)}. \tag{82}$$

This estimate of the steady-state drifting velocity of an object in regular waves is apparently new. It suggests that its magnitude and sign may be affected significantly by the wave-drift damping coefficient. Moreover the ideal fluid theory used to derive (82) suggests that the drifting velocity of a body in regular waves is independent of their amplitude! The quadratic rate of increase of the drift force with the wave amplitude is counterbalanced by the same rate of increase of the wave-drift damping force which opposes the drifting translation for a positive drift damping coefficient. When no external force is present to absorb momentum flux, the balance of these two counteracting effects leads to a drifting velocity which is independent of the wave amplitude.

A second interesting property of U is that it may become negative. The drift force $D(\omega_0)$ acting on a freely floating body is known to always point in the direction of wave propagation. For certain body geometries, the drift damping coefficient may however become negative over a certain frequency range. In such cases the object would tend to translate in a direction opposite to that of the wave propagation! This is the case for an array of four circular cylinders over certain frequency intervals.

Figure 7 illustrates the drifting velocity of a single cylinder as a function of va. Its positive magnitude indicates that the cylinder drifts in the direction of the wave propagation. The drifting velocity of the four-cylinder configuration is illustrated in figure 8. Over certain frequencies it may be seen to become negative owing to the negative sign of the corresponding wave-drift damping coefficient illustrated in figure 4. Negative wave-drift damping coefficients were also computed in Nossen *et al.* (1991) for a realistic offshore structure including the effects of the body oscillations which have not been accounted for in the present study. Vanishing values of the wave-drift damping coefficient indicate that (at least to leading order in U) the drifting motion of the body is unopposed by ideal fluid effects. Over such frequencies, the present model predicts large values for the drifting velocity which may isolate the small-U assumption. Moreover, viscous effects have not been included in the potential flow model which led to (82). They are likely to affect significantly the magnitude and perhaps the sign of drifting velocity observed in practice.

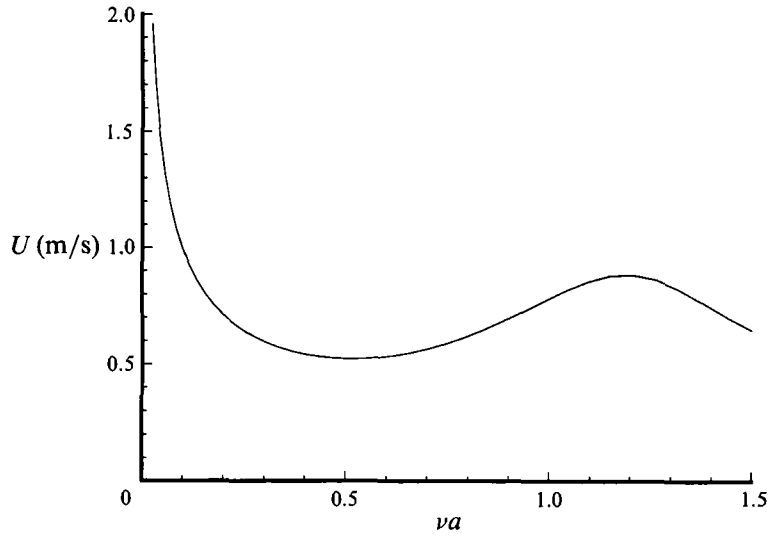

FIGURE 7. Drifting velocity of a single, vertical cylinder. The velocity is obtained for $\beta = 0$. Note that the drifting velocity U neither depends on the wave amplitude nor the cylinder radius for a given value of νa.

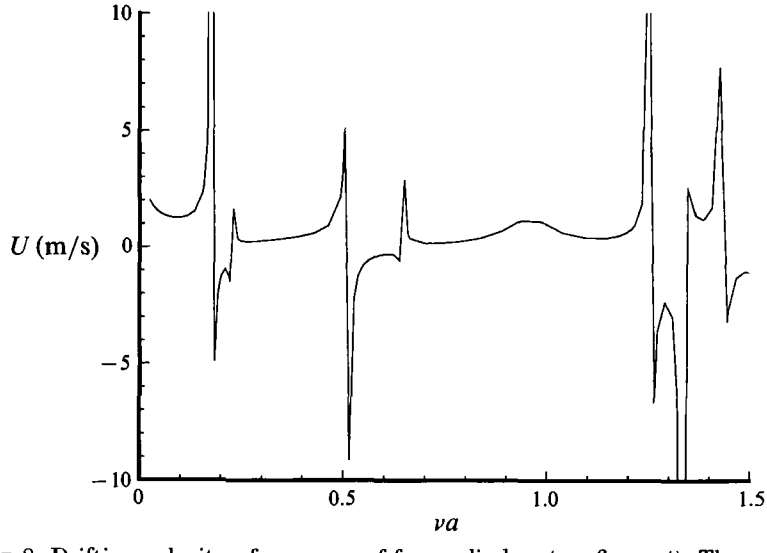

FIGURE 8. Drifting velocity of an array of four cylinders (see figure 4). The velocity is obtained for $\beta = 0$.

7. Concluding remarks

The rectilinear slow-drift oscillation of a floating body constrained by a weak restoring force in random waves has been studied. Ideal fluid effects only were considered, and the nonlinear free-surface flow was reduced to a series of linear and second-order problems under the assumption of a small wave slope and a slow-drift velocity small relative to the wave phase velocity. An ordinary differential equation governing the slow-drift response was derived which allows the evaluation of the second-order quadratic transfer matrices in the frequency domain independently of the slow-drift response which may be determined in the time domain.

Body geometries consisting of a single and arrays of vertical circular cylinders were considered. Explicit expressions were derived for the wave-drift damping coefficient by employing the McCamy and Fuchs solution for the single cylinder, and an exact interaction theory for multiple cylinders. Computations of the wave-drift damping coefficient for a rectangular configuration of cylinders revealed an oscillatory dependence upon the wave frequency which leads to negative drift damping coefficients over frequency intervals where wave interactions are significant.

A new expression has been derived for the drifting velocity of a body floating freely in regular waves. It was shown to be equal to the ratio of the drift force to the drift damping coefficient. Computations for a single cylinder restrained at its mean position suggested that its drifting velocity in regular waves points in the same direction as the direction of wave propagation. Analogous computations for a four-cylinder configuration suggested that a negative drifting velocity occurs over frequencies where wave interactions between the cylinders are strong.

A future study of the hydrodynamic problem in the frequency domain will include the solution of the radiation problem by employing the theoretical framework developed in this paper for the diffraction wave disturbance. The hydrodynamic coupling of the surge–sway–yaw slow-drift displacements will also be addressed owing to its relevance to practical applications.

An analogous effort must be devoted to the study of the slow-drift equation of motion and its extensions to all horizontal modes. Efficient numerical simulations in real wave spectra must be developed in parallel with the hydrodynamic analysis, in order to determine the statistical properties of the slow-drift responses and evaluate their sensitivity to ideal and viscous effects.

Financial support for this study has been provided by the MIT Sea Grant College Program, and it is greatly appreciated. Many thanks are also directed to Dr John Grue of the Department of Mathematics of Oslo University for providing us with the drift damping computations obtained from a three-dimensional panel method.

REFERENCES

ABRAMOWITZ, M. & STEGUN, I. A. 1972 *Handbook of Mathematical Functions*. Dover.

DAVIES, B. 1978 *Integral Transforms and Their Applications*. Springer.

FALTINSEN, O. M. 1990 *Sea Loads on Ships and Offshore Structures*. Cambridge University Press.

HERMANS, A. J. 1991 Slowly moving hull forms in short waves. *J. Engng Maths* **25**, 63–75.

HUIJSMANS, R. H. M. & HERMANS, A. J. 1985 A fast algorithm for computation of 3-D ship motions at moderate forward speed. In *4th Intl Conf. on Numerical Ship Hydrodynamics*.

LINTON, C. M. & EVANS, D. V. 1990 The interaction of waves with arrays of vertical circular cylinders. *J. Fluid Mech.* **215**, 549–569.

MARUO, H. 1960 Wave resistance of a ship in regular head sea. *Bull. Faculty Engng, Yokohama Natl Univ.*, vol. 9.

NEWMAN, J. N. 1967 The drift force and moment on ships in waves. *J. Ship Res.* **11**, 51–60.

NOSSEN, J., GRUE, J. & PALM, E. 1991 Wave forces on three-dimensional floating bodies with small forward speed. *J. Fluid Mech.* **227**, 135–160.

WU, G. X. & EATOCK-TAYLOR, R. 1990 The hydrodynamic force on an oscillating ship with low forward speed. *J. Fluid Mech.* **211**, 333–353.

ZHANO, R. & FALTINSEN, O. M. 1988 Interaction between waves and current on a 2-D body in the free surface. *Appl. Ocean Res.* **10**, 87–99.

ZHAO, R. & FALTINSEN, O. M. 1989 Interaction between current, waves and marine structures. In *5th Intl Conf. on Numerical Ship Hydrodynamics*.